Two-dimensional Wigner crystal of electrons on a helium film: Static and dynamical properties

F. M. Peeters*
AT&T Bell Laboratories, Murray Hill, New Jersey 07974
(Received 28 November 1983)

The interaction energy, phonon spectrum, and longitudinal and transverse sound velocity of a two-dimensional (2D) Wigner crystal are calculated within the harmonic approximation for different values of the thickness of the underlying helium film and for different types of substrates which support the He film. The phase diagram for Wigner crystallization is analyzed in terms of the Kosterlitz-Thouless-Halperin-Nelson theory of 2D melting.

I. INTRODUCTION

During the last decade two-dimensional (2D) electrons have been the subject of intense interest,[1] e.g., electrons in metal-oxide-semiconductor (MOS) structures and electrons on a He surface. Electrons in MOS structures behave mainly quantum mechanically (Fermi energy $E_F \sim 10-500$ K) because of their relatively high density $n_s \sim 10^{11}-10^{13}$ cm^{-2}. Lowering the electron density leads to trapping of the electrons by impurities. On the other hand, electrons on bulk helium form the opposite limit; they behave classically ($E_F \sim 0.01-100$ mK) with a density range of 10^5-10^9 cm^{-2}. Bulk He films become unstable when the electron density exceeds 2.4×10^9 cm^{-2}. But if one decreases the He-film thickness it is possible[2] to charge the He surface to a higher electron density; e.g., for a He-film thickness of $d \cong 100$ Å the He surface can support an electron density of about 10^{11} cm^{-2} (see Appendix), and one can enter the quantum regime. We expect that electrons on He films can form an interesting experimental system which bridges the gap between the classical (i.e., electrons on bulk He) and the pure quantum-mechanical (i.e., electrons in MOS structures) 2D electron systems known to date.

An interesting feature of the system of electrons above a helium film is that it can form a 2D Wigner lattice. Such a 2D crystallization was proposed by Crandall and Williams[3] and experimentally observed first by Grimes and Adams[4] and later in other studies.[5] All these experiments[4,5] were done for electrons on bulk helium. In the present paper we will apply Lindeman's melting criterium[6] as used by Platzman and Fukuyama[7] to investigate the influence of the thickness of the helium film on the phase transition for Wigner crystallization. An outline of such a study was presented in Ref. 8.

A particular aspect of the system of electrons on a helium film is the possibility of changing the interparticle interaction. Because of the finite distance between the electron layer and the substrate the electron-electron interaction is screened by the substrate. This screening effect can drastically change the interparticle potential, e.g., for a metallic substrate and a helium-film thickness smaller than the average electron-electron distance, the electron electron interaction becomes a dipole-dipole interaction. Classical aspects of such a dipole system were considered in Ref. 9. In the present paper we discuss the electron-helium film-substrate system for an arbitrary helium film thickness and an arbitrary substrate dielectric constant. We find that the dipole system exists only in certain limits.

The paper is organized as follows. An estimation of the phase diagram for 2D Wigner crystallization as a function of the helium-film thickness is given in Sec. II in terms of dimensionless units. In Sec. III we use the harmonic approximation to calculate the interaction energy and the phonon spectrum for a 2D layer of electrons crystallized in a hexagonal Wigner lattice. The effects of the He-film thickness and of the substrate dielectric constant on these properties are obtained. In the Conclusion we discuss the implication of the screening effects on the phase diagram for 2D Wigner crystallization. The stability of a helium film charged with electrons is discussed in the Appendix.

II. PHASE DIAGRAM

The electrostatic interaction energy between two electrons above a He film which lies on a substrate with dielectric constant ϵ is

$$V(r)=e^2\left[\frac{1}{r}-\frac{\delta}{[r^2+(2d)^2]^{1/2}}\right] \tag{1}$$

with $\delta=(\epsilon-1)/(\epsilon+1)$, and d is the distance between the electron layer and the substrate (d is approximately the He-film thickness). Notice that for a metallic substrate $\epsilon=\infty$ and thus $\delta=1$. The second term in Eq. (1) is a consequence of the screening of the interparticle interaction due to the substrate. For small interparticle distances ($r \ll d$) the screening is negligible and one has essentially a Coulombic potential: $V(r)=e^2/r+\cdots$. If, on the other hand, the electrons are far apart ($r \gg d$) we have $V(r)=e^2(1-\delta)/r+2\delta e^2d^2/r^3+\cdots$, which implies that for a nonmetallic substrate the charge is renormalized to an effective charge $e^*=e\sqrt{1-\delta}$. If $\delta=1$, then the interparticle interaction is dipolar at large distances. This shows clearly that by changing the He-film thickness the interparticle interaction can be changed. For a metallic substrate even the type of interaction can be changed from

a Coulombic to a dipolar one.

In the next section we need the Fourier transform of the interparticle potential [Eq. (1)]

$$v(k)=\frac{2\pi e^2}{k}(1-\delta e^{-2dk}) , \tag{2}$$

which has the following limiting behavior:

$$v(k)=2\pi e^2/k+\cdots \quad \text{for } dk\gg 1$$

and

$$v(k)=2\pi e^2(1-\delta)/k+4\pi\delta e^2 d+\cdots \quad \text{for } dk\ll 1 .$$

Lindeman's melting criterion[6,7] tells us that melting occurs when the kinetic energy exceeds the potential energy with a fraction $1/\Gamma$. Thus $\Gamma=\langle V\rangle/\langle K\rangle$ determines the phase diagram. In a qualitative picture the average potential energy [see Eq. (1)] is

$$\langle V\rangle=e^2\sqrt{\pi}\sqrt{n}\left[1-\frac{\delta}{(1+n/n_d)^{1/2}}\right] \tag{3}$$

with $n=1/\pi r_0^2$ the electron density and $n_d=1/4\pi d^2$. The kinetic energy of the 2D electron system is

$$\langle K\rangle=\frac{2}{n}\int\frac{d^2p}{(2\pi)^2}\frac{E_p}{e^{\beta(E_p-\mu)}+1} \tag{4}$$

with $E_p=p^2/2m$, $\beta=1/k_BT$, where k_B is Boltzmann's constant and T the temperature, and where the chemical potential μ is determined by the normalization condition

$$n=2\int\frac{d^2p}{(2\pi)^2}\frac{1}{e^{\beta(E_p-\mu)}+1} . \tag{5}$$

It is convenient to introduce the density

$$n_c=\frac{4}{\pi a_B^2}\frac{1}{\Gamma^2}=\frac{4e^4m^2}{\pi\hbar^4\Gamma^2} , \tag{6}$$

with $a_B=\hbar^2/me^2=0.529$ Å the Bohr radius, and the temperature

$$T_c=\frac{2e^2}{\Gamma^2}\frac{1}{k_Ba_B}=\frac{2me^4}{k_B\hbar^2\Gamma^2} . \tag{7}$$

For[4] $\Gamma=137$ we have $T_c=33.6$ K and $n_c=2.4\times10^{12}$ cm^{-2}.

Equations (3)–(5) can be written as

$$(n/n_c)^{1/2}=\frac{F_1^2(z)}{F_3^2(z)}\left[1-\frac{\delta}{(1+n/n_d)^{1/2}}\right] , \tag{8a}$$

$$(n/n_c)^{1/2}=\frac{T}{T_c}F_1(z) , \tag{8b}$$

with $F_1(z)=\frac{1}{2}\ln(1+1/z)$ and $F_3(z)=F_1^2(z)-s(1/(1+z))$, where

$$s(x)=-\int_0^x dy[(\ln|1-y|)/y]$$

is the dilogarithm and $z=e^{-\beta\mu}$. After eliminating z in Eqs. (8a) and (8b), we are left with a relation between the dimensionless densities $n/n_c, n_d/n_c$ and the temperature T/T_c which determines a surface in the three-dimensional (3D) space made up of $(n/n_c, n_d/n_c, T/T_c)$.

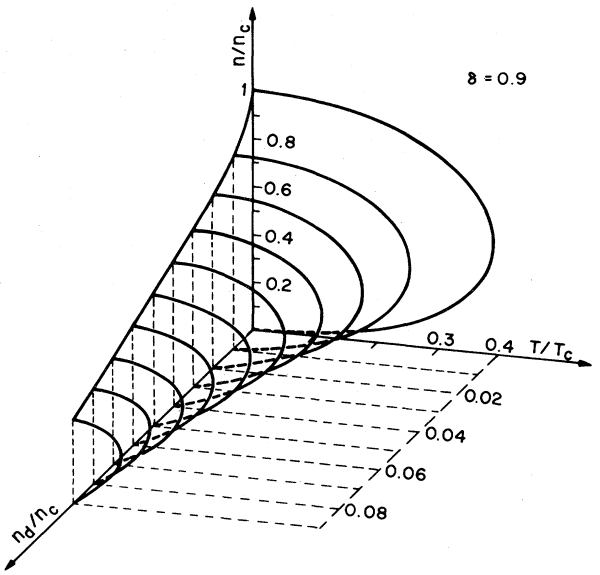

FIG. 1. Solid-liquid phase diagram for Wigner crystallization (inside the curves the 2D electron system is in the solid phase). $n_d=1/4\pi d^2$ with d being the distance between the electron layer and the substrate. This substrate is nonmetallic.

This phase diagram is plotted in Fig. 1 for a nonmetallic substrate and in Fig. 2 for a metallic substrate. For small He-film thicknesses (i.e., n_d/n_c large) both phase diagrams differ considerably. This is more apparent in Fig. 3 where we have plotted a $T=0$ cut of the phase diagram of Figs. 1 and 2.

The small-density–small-temperature region is of particular interest. For bulk He (i.e., $d=\infty$) this region corresponds with the classical regime (i.e., $\langle K\rangle=k_BT$). For finite d this is only true if $\delta\neq1$. Let us first discuss the $\delta\neq1$ case. Above we found that decreasing d to 0 results only in a renormalization of the charge, and this results in

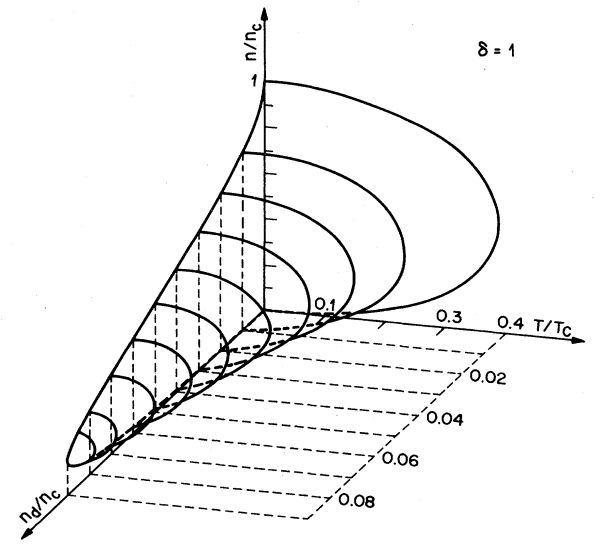

FIG. 2. Same as Fig. 1 but for metallic substrate.

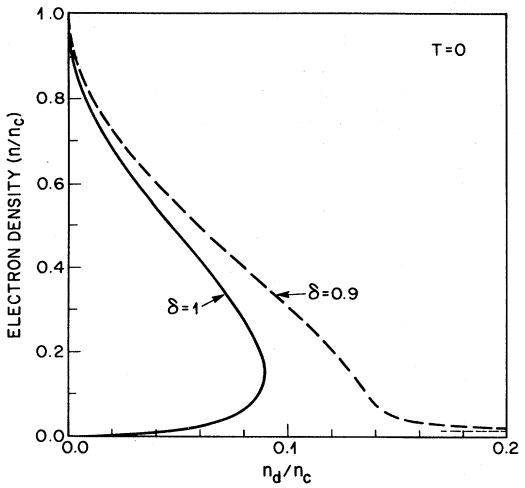

FIG. 3. $T=0$ cut of the phase diagrams of Figs. 1 and 2.

a renormalization of n_c and T_c. Explicitly $n_c \to n_c^* = (1-\delta)^2 n_c$, $T_c \to T_c^* = (1-\delta)^2 T_c$, which results in a shrinking of the phase diagram. Thus for $\delta=0.1$ we have $n/n_c \to 0.01$ and $T/T_c \to 0.01$ if $d \to 0$.

For $\delta=1$ and finite d the situation is totally different in the low-temperature region. For $n \ll n_d$ the potential energy behaves as $\langle V \rangle \sim d^2 n^{3/2}$, while the kinetic energy $\langle K \rangle \sim n$ in the quantum regime. This implies that for sufficiently small densities one has $\langle V \rangle \ll \langle K \rangle$, and the system is in the liquid state. For $n \gg n_d$, $\langle V \rangle \sim \sqrt{n}$ and thus for high densities we have again $\langle V \rangle \ll \langle K \rangle$, and the system is in the liquid state. Thus at a fixed temperature the Wigner lattice can only exist for $n_1 < n < n_2$, where n_1 and n_2 are a function of the He-film thickness. For example $n_1 = 4(n_d/n_c)^2$, $n_2 = 1 - 2(n_d/n_c)^{1/2}$ if $T=0$ and $n_d/n_c \ll 1$. Remember that for $\delta \neq 1$, $n_1 = 0$ for $T=0$ because a classical limit exists, while for $\delta=1$ the system is always quantum mechanical for $T \to 0$. With decreasing He-film thickness n_1 and n_2 move to each other and for $d = d^*$ (we found $n_d/n_c = 0.0901$, which implies $d^* = 60.4$ Å if $\Gamma = 137$) we have $n_1 = n_2 = n^*$. For $d < d^*$ no solid phase exists (see Figs. 2 and 3).

III. INTERACTION ENERGY AND PHONON SPECTRUM

In this section we study the properties of the 2D electron system when it is crystallized into a two-dimensional solid. The static interaction energy and the vibrational spectrum will be calculated in the harmonic approximation

The interaction energy of one electron, which is taken at the origin for convenience, interacting with all the other electrons is

$$E_I^e = \sum_{l \neq 0} V(\vec{R}(l)) , \tag{9}$$

which is identical to

$$E_I^e = \lim_{|\vec{R}| \to 0} \sum_l [V(\vec{R} - \vec{R}(l)) - V(\vec{R})] , \tag{10}$$

where $\vec{R}(l)$ is the lattice position of the electron at site l and $V(\vec{R})$ is given by Eq. (1). The sum in Eq. (9) runs over all possible lattice sites l except the origin. Because the lattice sum is slowly convergent, it is advisable to use the Ewald method which converts the sum in Eq. (10) into two rapidly converging sums. In the Ewald method[10,11] one separates the lattice sum into a part which contains the short distance interactions and a part which contains the long distance interactions. The latter sum is then transformed into Fourier space.

For $\delta \neq 1$, nonmetallic substrate, the energy E_I^e is divergent. This is a consequence of the fact that the Fourier transform of the interparticle interaction [see Eq. (2)] diverges for $k \to 0$. We will subtract the contribution of the $k=0$ mode, E_I^0, and consider

$$E_I = E_I^e - E_I^0 ,$$

which amounts to making the system charge neutral.[11] For the system under study we found

$$\frac{E_I}{E_0} = -\frac{2\pi}{\alpha} d_0 + \frac{2\sqrt{\pi}}{\alpha\eta} L_\delta(0, \eta^2 d_0^2) + \frac{2\sqrt{\pi}}{\alpha\eta} \sum_{\vec{G} \neq \vec{0}} L_\delta \left[\frac{G_0^2}{4\eta^2}, \eta^2 d_0^2 \right] + \left[-\frac{2\eta}{\sqrt{\pi}} + \delta \frac{\operatorname{erf}(\eta d_0)}{d_0} \right]$$
$$+ \sum_{\vec{R} \neq \vec{0}} \left[\frac{\operatorname{erfc}(\eta |\vec{R}_0|)}{|\vec{R}_0|} - \delta \frac{\operatorname{erfc}[\eta(|\vec{R}_0|^2 + d_0^2)^{1/2}]}{(|\vec{R}_0|^2 + d_0^2)^{1/2}} \right] \tag{11}$$

with $E_I^0 = 2\pi d_0/\alpha$, $\eta = \sqrt{\pi\zeta/\alpha}$, $d_0 = d/b$, $G_0 = Gb$, $E_0 = b/e^2$, b is the lattice constant, $\alpha = a_c/b^2$ with a_c the volume of the unit cell,

$$L_\delta(z,t) = \int_0^1 \frac{dx}{x^{3/2}} (1 - \delta e^{-xt}) e^{-z/x} , \tag{12}$$

$\operatorname{erf}(x)$ the error function, and $\operatorname{erfc}(x) = 1 - \operatorname{erf}(x)$ the complementary error function. ζ is an arbitrary constant which indicates at which distance the lattice sum is split. For a hexagonal lattice we have $\alpha = \sqrt{3}/2$, $b = (2\pi/\sqrt{3})^{1/2} r_0$, the normalized lattice vectors are $\vec{R}_0 = (m + n/2, \sqrt{3}n/2)$ and the normalized reciprocal-lattice vectors are given by $\vec{G}_0 = 2\pi(m, (-m+2n)/\sqrt{3})$ with $m,n = 0,1,2,\ldots$.

We have checked that for all values of the He-film thickness the hexagonal lattice structure gives a lower interaction energy than the square and centered rectangular lattice structure. For $d \to \infty$ (bulk helium), Eq. (11) reduces to the result

of Bonsall and Maradudin [Eq. (2.12) of Ref. 11]. This is easily seen if one recalls that

$$L_\delta(z,\infty)=\tfrac{1}{2}\sqrt{\pi/z}\,\mathrm{erfc}(\sqrt{z})=\tfrac{1}{2}\phi_{-1/2}(z)\ , \tag{13}$$

where $\phi_\nu(z)$ is the Misra function.

The interaction energy of the electron in the hexagonal 2D Wigner lattice is plotted in Fig. 4 as function of the distance between the electron layer and the substrate and for substrates with different dielectric constants. With decreasing He-film thickness the interaction energy decreases because of the enhanced screening of the interparticle interaction due to the substrate. For $d\to 0$ we have $e\to e\sqrt{1-\delta}$, which implies that E_I at $d=0$ differs with a factor $1-\delta$ with E_I at $d=\infty$, as is clearly apparent from Fig. 4.

In the second part of this section the phonon spectrum of the 2D Wigner crystal will be calculated in the harmonic approximation. Following Ref. 11 we define the matrix

$$S_{ij}(\vec{q})=\frac{1}{e^2}\lim_{|\vec{R}|\to 0}\frac{\partial^2}{\partial R_i\partial R_j}\left[\sum_l V(\vec{R}-\vec{R}(l))e^{-i\vec{q}\cdot\vec{R}(l)}-V(\vec{R})\right] \tag{14}$$

from which one can obtain the dynamical matrix

$$C_{ij}(\vec{q})=-\frac{e^2}{m}[S_{ij}(q)-S_{ij}(0)] \tag{15}$$

and the normal-mode frequencies

$$\omega_\pm^2(q)=\tfrac{1}{2}([C_{xx}(q)+C_{yy}(q)]\pm\{[C_{xx}(q)-C_{yy}(q)]^2+4C_{xy}(q)C_{yx}(q)\}^{1/2})\ . \tag{16}$$

Inserting the potential (1) into Eq. (14) and using the Ewald method as before we find for the dynamical matrix

$$\begin{aligned}C_{ij}(q)/\omega_0^2=&\frac{1}{2\eta}\sqrt{\pi/3}q_{0i}q_{0j}L_\delta\left[\frac{q_0^2}{4\eta^2},\eta^2d_0^2\right]-\frac{\eta^3}{2\sqrt{\pi}}\sum_{\vec{R}\neq\vec{0}}\sin^2(\tfrac{1}{2}\vec{q}_0\cdot\vec{R}_0)(\delta_{ij}\{H_1(\eta R_0)-\delta H_1[\eta(R_0^2+d_0^2)^{1/2}]\}\\&-v^2R_{0i}R_{0j}\{H_2(\eta R_0)-\delta H_2[\eta(R_0^2+d_0^2)^{1/2}]\})\\&+\frac{1}{2\eta}\sqrt{\pi/3}\sum_{G\neq 0}\left[(\vec{q}_0+\vec{G}_0)_i(\vec{q}_0+\vec{G}_0)_jL_\delta\left[\frac{|\vec{q}_0+\vec{G}_0|^2}{4\eta^2},\eta^2d_0^2\right]-G_{0i}G_{0j}L_\delta\left[\frac{|\vec{G}_0|^2}{4\eta^2},\eta^2d_0^2\right]\right],\end{aligned} \tag{17}$$

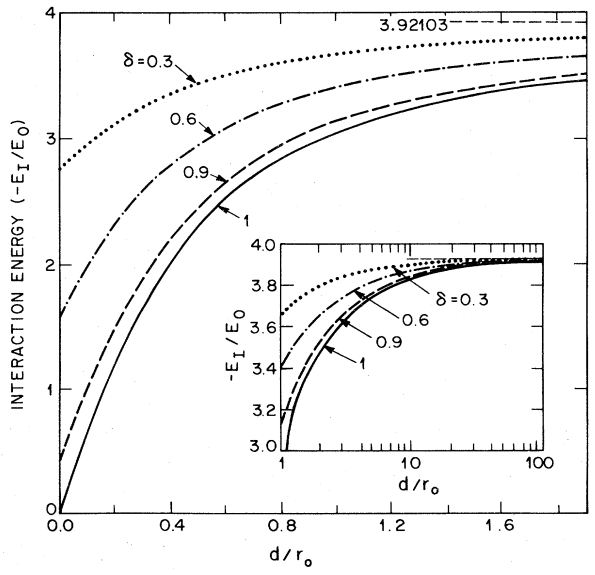

FIG. 4. Electron interaction energy as function of the relative film thickness (r_0 is the average electron-electron distance) for different substrates.

with $\omega_0^2=8e^2/mb^3$, $\vec{q}_0=\vec{q}b$,

$$H_1(x)=\frac{1}{x^2}\left[\frac{\sqrt{\pi}}{2}\frac{\mathrm{erfc}(x)}{x}+e^{-x^2}\right], \tag{18a}$$

$$H_2(x)=\frac{1}{x^2}\left[\frac{3}{2}\sqrt{\pi}\frac{\mathrm{erfc}(x)}{x^3}+3\frac{e^{-x^2}}{x^2}+2e^{-x^2}\right], \tag{18b}$$

and the summations are over the same lattice vectors as in Eq. (11). If one observes that $H_1(x)=\phi_{1/2}(x^2)$ and $H_2(x)=2\phi_{3/2}(x^2)$ then it is easy to show that in the limit $d\to\infty$, Eq. (17) reduces to Eq. (3.10) of Ref. 11. In the case of a metallic substrate ($\epsilon=\infty$) the present results are equivalent to the results of Meissner *et al.*[12] for the electron vibrational excitations in a three-layer structure.

The phonon spectrum is plotted in Fig. 5 along the boundary of the irreducible element of the first Brillouin zone[11] for different values of the He-film thickness and for two different substrates: a nonmetallic substrate [Fig. 5(a)] and a metallic substrate [Fig. 5(b)]. The longitudinal C_l and transverse C_t sound velocity are shown in Fig. 6 as a function of d. From Figs. 5(a), 5(b), and (6) it is apparent that (1) the screening effects are starting to play a role when $d/r_0\leq 1$, i.e., when the distance between the

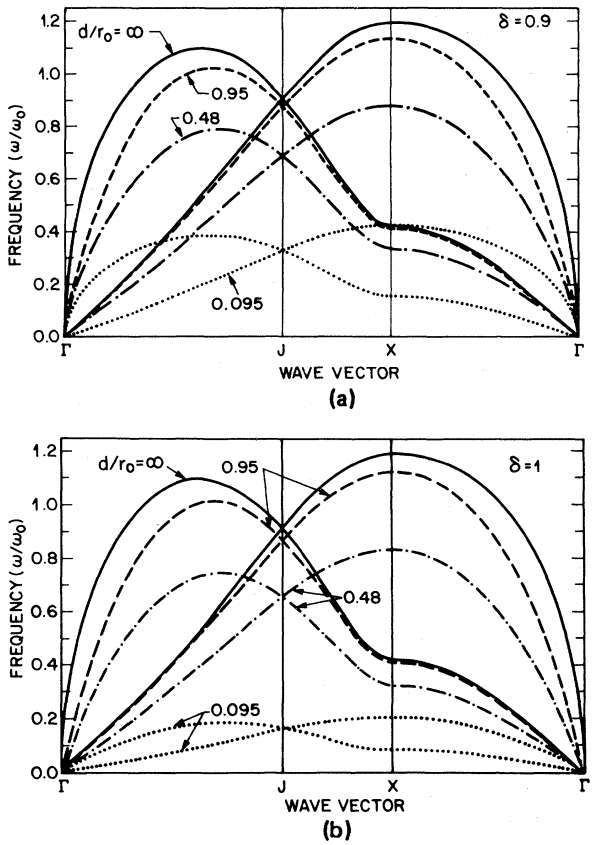

FIG. 5. Phonon spectrum in the case of (a) a nonmetallic and (b) a metallic substrate along the boundaries of the irreducible element of the first Brillouin zone for different values of the relative film thickness. $\omega_0^2=8e^2/mb^3$ with b the lattice vector.

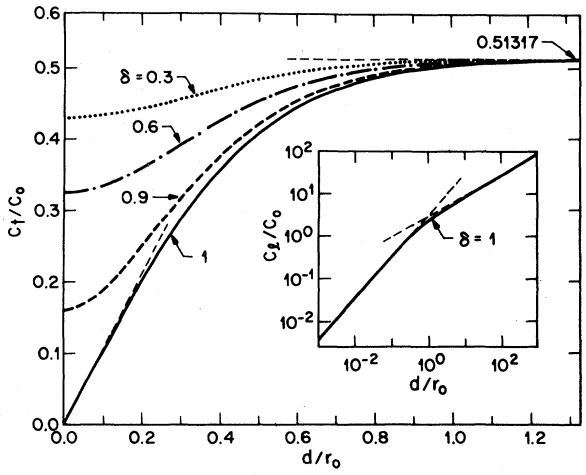

FIG. 6. Transverse (C_t) and longitudinal (C_l) sound velocity as function of the relative film thickness for different substrates. $C_0^2=e^2/mb$.

electron layer and the substrate is comparable to or smaller than the average distance between the electrons in the crystal. Decreasing the film thickness and/or increasing the dielectric constant of the substrate softens the phonon spectrum. (2) For a nonmetallic substrate the longitudinal sound velocity is always infinity. The reason is that for $\delta\neq 1$ the 2D electron system behaves, in the long-wavelength limit, as a Coulomb system and thus, as is well-known, $\omega_l\sim q^{1/2}$ for $q\to 0$. For the case of a metallic substrate and $d/r_0<\infty$ the two branches of the phonon spectrum are acoustical in the long-wavelength limit, i.e., $\omega\sim q$ for $q\to 0$. For $\delta=1$ the system behaves, in the $q\to 0$ limit, as a series of dipoles. This explains why $\omega_l\sim q$ as $q\to 0$. (3) Notice the superlinear behavior of the transverse mode if $d/r_0\geq 0.5$. This was already observed in Ref. 11 in the case of a 2D Wigner lattice on bulk helium. (4) The sound velocities as a function of the film thickness have the following limits. (i) for a metallic substrate ($\delta=1$)

$$C_l/C_0=\begin{cases}2.760(d/r_0)^{1/2}, & d/r_0\gg 1 \quad (19a)\\ 3.542\,d/r_0, & d/r_0\ll 1 \quad (19b)\end{cases}$$

$$C_t/C_0=1.068\,d/r_0,\quad d/r_0\ll 1 \quad (19c)$$

with $C_0^2=e^2/mb$. (ii) For a nonmetallic substrate with $\delta=0.9$

$$C_t/C_0=0.162\,28+3.14(d/r_0)^2,\quad d/r_0\ll 1 \quad (19d)$$

and in general

$$\lim_{d\to 0} C_t/C_0=0.513\,17\sqrt{1-\delta}\,. \quad (19e)$$

In the limit of bulk helium we have the well-known result[11] $C_t/C_0=0.513\,17$.

IV. CONCLUSION

In Sec. II the phase diagram (Figs. 1 and 2) was presented in terms of variables which were scaled by the renormalization constants n_c and T_c. These constants depend on the parameter Γ which contains information about the interactions in the system. Thus we expect that Γ will be a function of the He-film thickness.

For bulk He and for small temperature ($T<1$ K, i.e., the classical regime) Thouless[13] used the Kosterlitz-Thouless[14] (KT) theory of dislocation-mediated melting, as elaborated in greater detail by Halperin and Nelson[15] and Young,[16] to estimate Γ. He obtained

$$\Gamma_{\rm KT}=\frac{\chi}{(C_t/C_0)^2(1-C_t^2/C_l^2)} \quad (20)$$

with $\chi=2^{3/2}3^{1/4}\pi^{3/2}=20.728$ and $C_0^2=e^2/mb$ with b the lattice constant and m the electron mass. For bulk He one has $C_t/C_0=0.513$, $C_l=\infty$, and thus[15] $\Gamma_{\rm KT}=79$. Morf[17] showed that the experimental[4] value $\Gamma\cong 137$ can be explained if the temperature dependence of the sound velocity C_t is taken into account.

To obtain an idea of the film thickness dependence of Γ we take

$$\frac{\Gamma_{\rm KT}(d)}{\Gamma_{\rm KT}(\infty)}=\frac{[C_t(\infty)/C_t(d)]^2}{1-[C_t(d)/C_l(d)]^2}\,, \quad (21)$$

where $\Gamma_{KT}(\infty)=137$ and use zero-temperature values of the sound velocity as obtained in the preceding section. The validity of Eq. (21) in the quantum regime is questionable. At most we may expect that it will give us a qualitative picture.

Taking into account the d dependence of Γ we have calculated from Eqs. (8a) and (8b) the phase diagram for Wigner crystallization in dimensional units. For a metallic substrate this was shown in Fig. 4 of Ref. 8. For a nonmetallic substrate with $\delta=0.9$ the phase diagram is shown in Fig. 7 for different values of the He-film thickness. The closed circle on each line indicates where the He surface becomes unstable (see Appendix).

Experimentally[18] it is easier to keep the electron density constant and change the He-film thickness. Therefore we plotted in Fig. 8 the phase diagram as function of the He-film thickness for three values of the electron density and for the case of a metallic and a nonmetallic substrate ($\delta=0.9$).

Figures 7 and 8 show that the screening effects become visible for $d \lesssim 10^4$ Å. For thin He films the solid-liquid boundary is pushed into the quantum regime. For a typical temperature of $T=0.4$ K, Fig. 7 suggests that the phase transition will begin to show quantum behavior when the film thickness becomes smaller than about 200 Å.

In summary, we have studied the interaction energy, the phonon spectrum, and the phase diagram for Wigner crystallization of a 2D system of electrons on a He film. Such a system forms an almost ideal 2D fermion system which provides the possibility of studying the transition from a classical 2D to a quantum 2D electron system. We expect that the analysis of the phase diagram presented in this paper is only an estimate when $E_F > kT$. The reason is that the calculation of $\Gamma_{KT}(d)$ was based on the

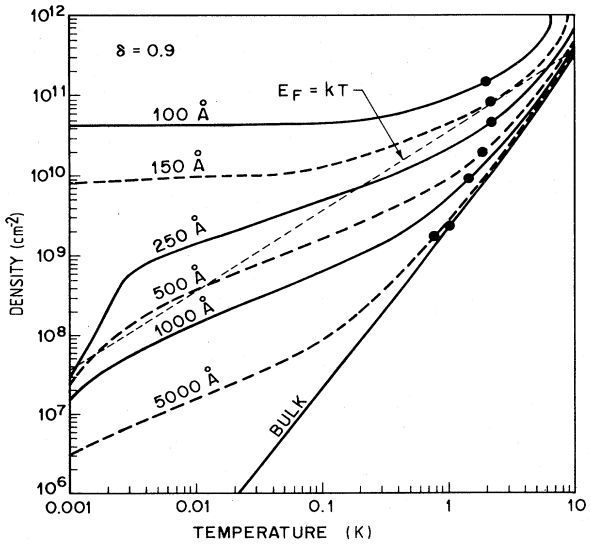

FIG. 7. Phase diagram for a nonmetallic substrate for different values of the film thickness. Closed circles are the stability points for the film.

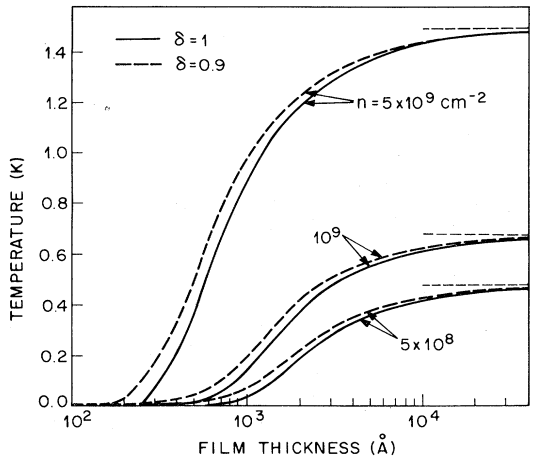

FIG. 8. Phase diagram as function of the film thickness for different values of electron density and for a metallic (solid curve) and a nonmetallic (dashed curve) substrate.

Kosterlitz-Thouless[14] theory of 2D melting, which is a classical theory. Up to now no quantum analog exists for the KT theory of 2D melting.

ACKNOWLEDGMENTS

I would like to thank E. Andrei, C. C. Grimes, Y. Iye, S. A. Jackson, and P. M. Platzman for stimulating discussions. This work was supported in part by the National Fonds voor Wetenschappelijk Onderzoek (Belgium), Fonds voor Kollektief Fundamenteel Onderzoek (FKFO) (Project No. 2.0072.80, Belgium) and North Atlantic Treaty Organization (NATO).

APPENDIX

In Ref. 2 (see also Ref. 19) the dispersion relation for He surface excitations of a He film of thickness d, which was charged with electrons (density n), was obtained:

$$\omega_k^2 = k\left[\left[\frac{3\alpha}{\rho d^4}+g\right]+\frac{\tau}{\rho}k^2-\frac{4\pi e^2 n^2}{\rho}k\frac{1+\delta e^{-2kd}}{1-\delta e^{-2kd}}\right] \times\tanh(kd)\,, \tag{A1}$$

where $\delta=(\epsilon-1)/(\epsilon+1)$ with ϵ the dielectric constant of the substrate beneath the He film, $\rho=0.145$ g cm^{-3} is the He mass density, $\tau=0.378$ erg cm^{-2} the He surface tension, g the gravitational constant, and we took $\alpha=9.5\times10^{-15}$ erg for the van der Waals coupling constant of the He to the substrate. Details of the derivation of (A1) and results in the limit of small He film thickness can be found in Ref. 2. In this Appendix we elaborate on the properties of this function (A1) for arbitrary He film thickness.

For electron densities larger than a certain critical density the He surface excitation frequency ω_k contains an imaginary term for a certain range of wave vectors which implies that for those electron densities the He surface is

unstable. The critical density (n^*) and corresponding critical wave vector (k^*) are obtained from the equations $\omega_k=0$, $\partial\omega_k/\partial k=0$, and are plotted in Fig. 9 as function of the He-film thickness and for a metallic ($\epsilon=\infty$) and a nonmetallic (i.e., $\epsilon=10$) substrate.

The limiting behavior of the critical density and critical wave vector are as follows (the He-film thickness d is in cm): (1) for thick He films ($d>10^7$ Å), one had $k^*d\gg1$ and thus

$$n^*=\left[\frac{\tau}{4\pi^2e^4}\left[\rho g+\frac{3\alpha}{d^4}\right]\right]^{1/4}=2.25\times10^{+9}\,, \tag{A2}$$

$$k^*=\frac{2\pi e^2(n^*)^2}{\tau}=19.4 \tag{A3}$$

(with n^* measured in cm^{-2} and k^* in cm^{-1}), which is independent of the dielectric constant of the substrate. (2) for thin He films and (i) a metallic substrate, $k^*=0$ for $d<8.9\times10^6$ Å and thus one can use the property $kd\ll1$ to obtain

$$n^*=\left[\frac{3\alpha}{4\pi e^2}\right]^{1/2}d^{-3/2}=99.2d^{-3/2}\,, \tag{A4}$$

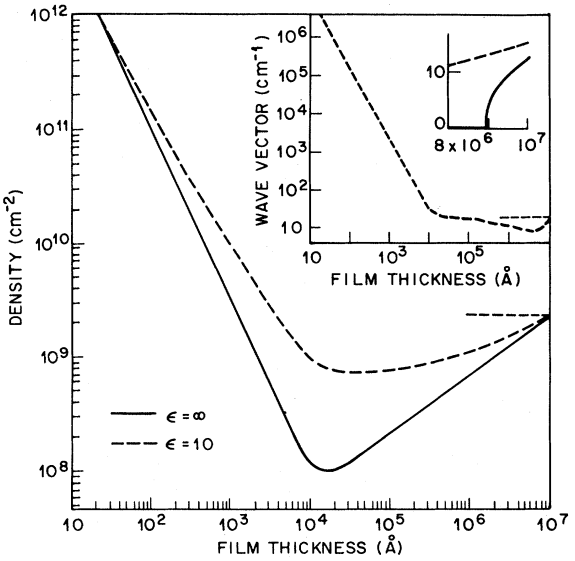

FIG. 9. Maximum electron density that a helium surface can support and the wave vector (inset) of the instability as a function of the He film thickness for both a metallic (solid curve) and a nonmetallic (dashed curve) substrate.

which is valid for $d<10^3$ Å. (ii) For a nonmetallic substrate it turns out that $kd\ll1$ only when $10^3\le d\le10^5$ Å, which gives (with n^* in cm^{-2} and k^* in cm^{-1})

$$(n^*)^2=\frac{\rho g}{2\pi e^2}\cdot\frac{\epsilon^2-1}{\epsilon^2}\left[1+\frac{3\alpha}{\rho g}\frac{1}{d^4}\right]\left\{d+\left\{d^2+\frac{\epsilon^2}{(\epsilon^2-1)^2}\left[\tau/\rho g\left[1+\frac{3\alpha}{\rho g}\frac{1}{d^4}\right]\right]\right\}\right\}$$

$$=9.83\times10^{19}\frac{\epsilon^2-1}{\epsilon^2}\left[1+\frac{2\times10^{-16}}{d^4}\right]\left\{d+\left\{d^2+\frac{\epsilon^2}{(\epsilon^2-1)^2}\left[2.65\times10^{-3}\Big/\left[1+\frac{2\times10^{-16}}{d^4}\right]\right]\right\}\right\}\,, \tag{A5}$$

$$k^*=\frac{\epsilon}{\tau}\frac{2\pi e^2(n^*)^2}{1+d(\epsilon^2-1)\dfrac{4\pi e^2(n^*)^2}{\tau}}=\frac{3.83\times10^{-18}\epsilon(n^*)^2}{1+d(\epsilon^2-1)(n^*)^2 7.67\times10^{-18}}\,. \tag{A6}$$

When $d\le10^3$ Å or 10^7 Å $>d>10^5$ Å then k^*d is of order 1 and no simple expression for n^* or k^* is found.

*Permanent address: Departement Natuurkunde, Universitaire Instelling Antwerpen, Universiteitsplein 1, B-2610 Wilrijk, Belgium.

[1]T. Ando, A. B. Fowler, and F. Stern, Rev. Mod. Phys. 54, 437 (1982).
[2]H. Ikezi and P. M. Platzman, Phys. Rev. B 23, 1145 (1981).
[3]R. S. Crandall and R. Williams, Phys. Lett. A34, 404 (1971).
[4]C. C. Grimes and G. Adams, Phys. Rev. Lett. 42, 795 (1979).
[5]A. S. Rybalko, B. N. Esel'son, and Yu. Z. Kovdrya, Fis. Nisk. Temp. 5, 947 (1979) [Sov. J. Low Temp. Phys. 5, 450 (1979)]; G. Deville, F. Gallet, D. Marty, J. Poitrenaud, A. Valdés, and F. I. B. Williams, in *Ordering in Two Dimensions*, edited by S. K. Sinha (North Holland, New York, 1980), p. 309; R. Mehrota, B. M. Guenin and A. J. Dahm, Phys. Rev. Lett. 48, 641 (1982).
[6]F. Lindeman, Z. Phys. 11, 609 (1910).
[7]P. M. Platzman and H. Fukuyama, Phys. Rev. B 10, 3150 (1974).
[8]F. M. Peeters and P. M. Platzman, Phys. Rev. Lett. 50, 2021 (1983).
[9]W. Huang, J. Rudnick, and A. J. Dahm, J. Low Temp. Phys. 28, 21 (1977); K. B. Ma and J. C. Inkson, J. Phys. C 11, L411 (1978); Y. P. Monarkha and Y. Z. Kovdrya, Fis. Nisk. Temp. 8, 215 (1982) [Sov. J. Low Temp. Phys. 8, 107 (1982)].
[10]J. M. Ziman, *Principles of the Theory of Solids* (Cambridge University Press, Cambridge, 1964), p. 37.
[11]L. Bonsall and A. A. Maradudin, Phys. Rev. B 15, 1959 (1977).
[12]G. Meissner, H. Namaisawa, and M. Vess, Phys. Rev. B 13, 1370 (1976); G. Meissner, Surf. Sci. 73, 411 (1978).
[13]D. J. Thouless, J. Phys. C 11, L189 (1978).
[14]J. M. Kosterlitz and D. J. Thouless, J. Phys. C 6, 1181 (1973).
[15]B. I. Halperin and D. R. Nelson, Phys. Rev. Lett. 41, 121 (1978); 41, 519(E) (1978).
[16]P. Young, Phys. Rev. B 19, 1855 (1979).
[17]R. H. Morf, Phys. Rev. Lett. 43, 931 (1979).
[18]E. Y. Andrei, Phys. Rev. Lett. 52, 1449 (1984).
[19]L. P. Gor'kov and D. M. Chernikova, Pis'ma Zh. Eksp. Teor. Fis. 18, 119 (1973) [JETP Lett. 18, 68 (1973)]; D. M. Chernikova, Fis. Nisk. Temp. 2, 1374 (1976) [Sov. J. Low Temp. Phys. 2, 669 (1976)].